

Glycine functionalized alumina nanoparticles stabilize collagen in ethanol medium

S PRABHU, K CHEIRMADURAI, J RAGHAVA RAO and P THANIKAIVELAN* 

Central Leather Research Institute (Council of Scientific and Industrial Research), Adyar, Chennai 600 020, India

MS received 15 May 2015; accepted 9 September 2015

Abstract. The synthesis of glycine functionalized Al_2O_3 nanoparticles ($\text{Gly@Al}_2\text{O}_3$) by a simple two-step process employing sucrose as a template was reported. The functionalization of Al_2O_3 nanoparticles with glycine was confirmed by Fourier transformed infrared (FT-IR) spectroscopy, X-ray diffraction, high-resolution scanning electron microscopy (HRSEM) and energy-dispersive X-ray (EDX) analysis. The interaction of $\text{Gly@Al}_2\text{O}_3$ nanoparticles with collagen fibres was demonstrated using HRSEM, EDX, differential scanning calorimetry and FT-IR analysis. The thermal stability of collagen is enhanced to 74°C upon interaction with $\text{Gly@Al}_2\text{O}_3$ nanoparticles thereby suggesting applications in leather making, biomedicine and cosmetic fields.

Keywords. Nanoparticles; stabilization; protein; functionalization; thermal stability.

1. Introduction

Collagen is a naturally occurring skin protein in animal tissue [1]. Collagen, a building block of skin matrix, plays vital role in many applications including leather making, tissue engineering and cosmetics. The triple helical structure of collagen is stabilized by inter- and intra-molecular hydrogen bonding interactions [2]. Collagen will destabilize on exposure to heat or specific enzymes such as collagenase. Destabilization of collagen can be overcome by adopting several methods like chemical [3] or physical [4] crosslinking. Only very few metal salts and select organic molecules can stabilize the collagen matrix and improve its hydrothermal stability [5–7]. Industrial processes such as leather manufacturing involve usage of huge amount of water in different stages of tanning process. The used water after tanning process is contaminated by the presence of chromium(III) and many different chemicals used in leather processing. This contaminated water will cause environmental pollution and the chromium needs to be recycled [8]. Further, the availability of water is decreasing over the years and it has been estimated that 1.8 billion people will live in countries or regions with absolute water scarcity by 2025 AD [9]. To overcome this challenge, chromium-free, water-less [10,11] and other greener approaches are being developed. Although aluminium tanning is known, it is not widely practiced owing to its reversible reaction with collagen [7].

Stabilization of collagen using nanoparticles offers ideal platform for swapping not only chromium usage in tanning but also water medium [12,13] since most nanoparticles disperse well in organic solvents rather than in water. SiO_2 nanoparticles were used to crosslink the collagen and enhance the thermal stability significantly [14]. The use of functionalized iron oxide nanoparticles for collagen stabilization both in aqueous and non-aqueous media was in recent times [15,16]. Castaneda *et al* [17] reported the crosslinking of collagen using tiopronin-modified gold nanoparticles via 1-ethyl-3(3-dimethylaminopropyl)-carbodiimide (EDC). Functionalization of nanoparticles gains additional benefit due to stabilization, high dispersion in solvents and prevents uncontrolled agglomeration of the nanoparticles [18].

Herein, the synthesis of glycine functionalized Al_2O_3 ($\text{Gly@Al}_2\text{O}_3$) nanoparticles for the stabilization of collagen fibres in non-aqueous medium was reported. Glycine was chosen for the functionalization of Al_2O_3 nanoparticles due to its small size, bi-functional group and biodegradable nature. It is proposed that the carboxyl groups of glycine can easily adsorb on the surface of the nanoparticles and amino groups could interact with the collagen molecule [19]. Al_2O_3 was first synthesized using sucrose as a template and then it is functionalized with glycine. The prepared $\text{Gly@Al}_2\text{O}_3$ nanoparticles were characterized using Fourier transformed infrared (FT-IR), X-ray diffraction (XRD), thermogravimetric analysis (TGA), high-resolution scanning electron microscopic (HRSEM) and energy-dispersive X-ray (EDX) analysis. The $\text{Gly@Al}_2\text{O}_3$ nanoparticles were dispersed in ethanol and treated with collagen fibres for stabilization. The treated fibres were further characterized using FT-IR, HRSEM, EDX and differential scanning calorimetric (DSC) analysis.

* Author for correspondence (thanik8@yahoo.com; thanik@clri.res.in)

2. Materials and methods

2.1 Materials

The collagen fibres (hide powder) were prepared as described elsewhere [15]. Aluminium sulphate ($\text{Al}_2(\text{SO}_4)_3 \cdot 16\text{H}_2\text{O}$) was procured from Merck Ltd., India. Sucrose was procured from HiMedia Laboratories, India. Glycine was procured from SD Fine-Chem, India. All chemicals and reagents were analytical grade and used as such without further purification. Deionized and distilled water was used throughout the experiment.

2.2 Preparation of Al_2O_3 and glycine functionalized $\text{Al}_2\text{O}_3(\text{Gly@Al}_2\text{O}_3)$

Al_2O_3 was prepared according to the reported procedure [20] with modifications. Initially, 4.275 g (0.0125 mol) of sucrose (template) was dissolved in 50 ml distilled water. Then 7.864 g (0.0125 mol) of $\text{Al}_2(\text{SO}_4)_3 \cdot 16\text{H}_2\text{O}$ was added and stirred vigorously for 30 min at 30°C. Then, pH of the above mixture was adjusted to 7 using aq. NaOH solution and stirred for 1 h. The stirred mixture was then heated at 100°C to remove water and other volatiles. The resulting solid was then calcined at 600°C for 6 h to remove the template. The obtained solid particles (Al_2O_3) were washed with water thrice and once with ethanol and then dried at 100°C in hot air oven for 5 h. For the functionalization of Al_2O_3 , 250 mg glycine and 250 mg Al_2O_3 were mixed in 15 ml ethanol and stirred for 3 h at 30°C. The pH of the mixture was measured to be around 6.5. The mixture was centrifuged to obtain white solid particles. Particles were washed with ethanol thrice to remove the un-coated glycine. The obtained product ($\text{Gly@Al}_2\text{O}_3$) was then dried under vacuum for overnight. The products were stored in clean vial and characterized.

2.3 Interaction of $\text{Gly@Al}_2\text{O}_3$ with collagen

In a typical procedure, 10 mg (10 wt%) of $\text{Gly@Al}_2\text{O}_3$ nanoparticles were sonicated in 5 ml ethanol for 15 min to achieve complete dispersion of the nanoparticles in the solvent. Then, 100 mg of collagen fibres (hide powder) were added to the above mixture and stirred for 2 h. For comparison, pure Al_2O_3 nanoparticles were used instead of $\text{Gly@Al}_2\text{O}_3$ nanoparticles in the above procedure for finding out the efficacy of interaction with collagen. The samples were then investigated for thermal stability, structure and morphology analysis.

2.4 Characterization of materials

XRD measurements were recorded using a Rigaku Miniflex (II) desktop diffractometer (Ni filtered $\text{CuK}\alpha$ radiation with $\lambda = 0.154\ 060\ \text{nm}$) in the 2θ range from 10° to 80° with scan rate of 0.2 deg min^{-1} . XRD patterns were

compared with the Joint Committee on Powder Diffraction Standards (JCPDS) data for phase identification. TGA of the synthesized $\text{Gly@Al}_2\text{O}_3$ nanoparticles was carried out using TGA Q50 (V20.13 Build 39, TA Instruments). About 6 mg of the sample was heated under nitrogen atmosphere at a heating rate of 20°C min^{-1} . The analysis was carried out from 30 to 800°C. FT-IR spectra of the samples were recorded using Perkin Elmer instrument. The samples were ground with KBr and compressed to form pellets. The pellets were analysed in a single beam mode at the range of 400–4000 cm^{-1} with an average of four scans and 2 cm^{-1} resolution. HRSEM analysis was carried out using a FEI Quanta (FEG 200) microscope. Before analysis, the samples were coated with gold. DSC analysis of the wet samples was carried out using a NETZSCH (DSC 204) instrument with scan rate of 2°C min^{-1} .

3. Results and discussion

3.1 Characterization of Al_2O_3 and $\text{Gly@Al}_2\text{O}_3$

XRD patterns of Al_2O_3 and $\text{Gly@Al}_2\text{O}_3$ are shown in figure 1a. All the diffraction peaks of Al_2O_3 are in good agreement with cubic $\gamma\text{-Al}_2\text{O}_3$ (JCPDS no. 29-0063). The broad diffraction peaks in the pattern suggest that the particles are in nano-size. The diffraction patterns of $\text{Gly@Al}_2\text{O}_3$ clearly show the presence of both $\gamma\text{-Al}_2\text{O}_3$ and glycine. Indeed, most of the diffraction peaks of Al_2O_3 appear to be weak and masked with sharp and strong peaks of glycine. The peaks of glycine in the XRD pattern of $\text{Gly@Al}_2\text{O}_3$ nanoparticles can be assigned to γ -glycine, a thermodynamically stable form (JCPDS no. 06-0230) [21]. The crystallite size of the nanoparticles were quantitatively calculated using Scherrer's formula using full-width at half-maximum intensity (FWHM) of (400) phase for $\gamma\text{-Al}_2\text{O}_3$ [22]. The calculated sizes are 3.6 and 5.8 nm for Al_2O_3 and $\text{Gly@Al}_2\text{O}_3$, respectively.

FT-IR spectra of pure glycine, Al_2O_3 and $\text{Gly@Al}_2\text{O}_3$ are shown in figure 1b. Pristine Al_2O_3 nanoparticles show characteristic broad Al–O–Al and Al–O bands in the range of 500–800 cm^{-1} . The characteristic peaks of glycine at 1332 (ωCH_2), 1412 ($\nu_s\text{COO}^-$), 1503 ($\delta_s\text{NH}_3$) and 3169 ($\nu_s\text{NH}_3$) cm^{-1} are in agreement with the earlier report [19]. The signature peaks of γ -glycine corresponding to $-\text{COO}^-$ rocking, $-\text{COO}^-$ bending, CCN stretching and CH_2 rocking are seen at 500, 685, 890 and 930 cm^{-1} , respectively [21]. The $\text{Gly@Al}_2\text{O}_3$ nanoparticles exhibit characteristic peaks of both glycine and alumina as marked with lines and box in figure 1b. This observation confirms the functionalization of glycine on the surface of Al_2O_3 nanoparticles. The broad band between 3800 and 3000 cm^{-1} may be due to the hydrogen bonding present in the product.

HRSEM images of Al_2O_3 and $\text{Gly@Al}_2\text{O}_3$ nanoparticles at low and high magnifications are shown in figure 2. The Al_2O_3 nanoparticles seem to be very fine with spherical shape having an average particle size of $20 \pm 3\ \text{nm}$.

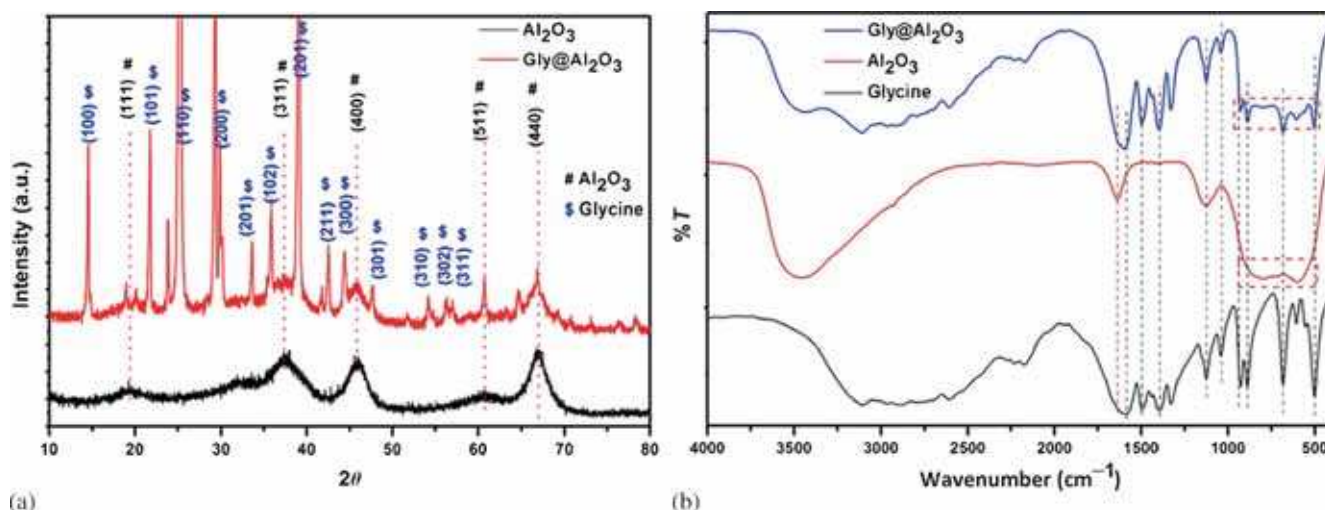


Figure 1. (a) XRD and (b) FT-IR spectra of Al₂O₃ and Gly@Al₂O₃ nanoparticles.

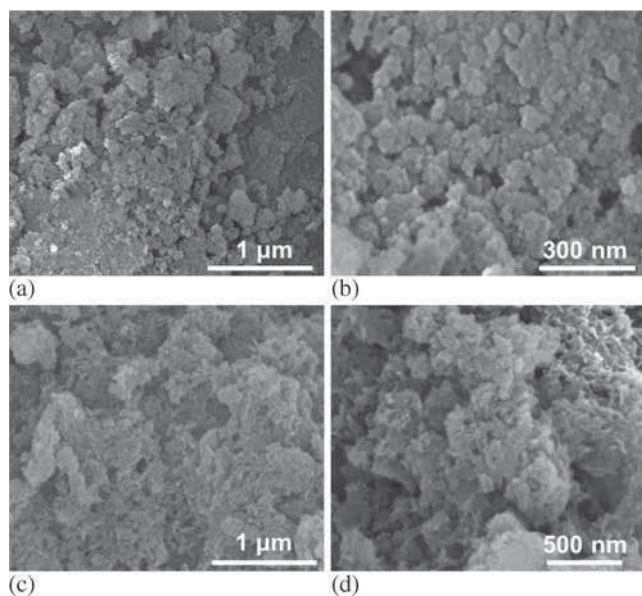


Figure 2. HRSEM images of Al₂O₃ nanoparticles at (a) lower and (b) higher magnifications and Gly@Al₂O₃ nanoparticles at (c) lower and (d) higher magnifications.

The higher size observed here in comparison to the value obtained in XRD results could be due to the gold coating on the particles as well as the agglomeration of the particles. In the absence of surface coating in Al₂O₃ nanoparticles, the attractive force between the nanoparticles increases due to the increase in the large surface area to volume ratio and the nanoparticles are agglomerated in order to reduce the surface energy [18]. HRSEM image of the Gly@Al₂O₃ nanoparticles shows that the particles are interconnected thereby forming layer or sheath-like structures rather than typical agglomeration. As the Al₂O₃ nanoparticles are functionalized through interaction of COO⁻ group in glycine

[19,23], agglomeration is prevented by the electrostatic repulsion of NH₃⁺ group in bi-functional glycine molecule between the Gly@Al₂O₃ nanoparticles. Nevertheless, the interionic interactions between the like-charged Gly@Al₂O₃ nanoparticles could attract individual particles and form layer or sheath-like structures [24]. Here, the individual particles are not difficult to visualize. This may be due to the presence of glycine on the surface of alumina nanoparticles, which lead to the weak interaction of one particle with the other through interionic interactions. The EDX spectra of Al₂O₃ and Gly@Al₂O₃ nanoparticles are shown in figure 3a and b, respectively. This confirms the presence of only Al and O for alumina nanoparticles while C, N, O and Al for Gly@Al₂O₃ nanoparticles. The peak around 2 eV in both the EDX spectra corresponds to gold arising from sample preparation for the HRSEM analysis.

3.2 Interaction of Gly@Al₂O₃ with collagen

Functionalization of Al₂O₃ nanoparticles with glycine was carried out at pH around 6.5, where glycine is in dipole or zwitterionic (⁺H₃N-CH₂-COO⁻) form. It is known that the interaction of glycine with Al₂O₃ nanoparticles is through COO⁻ group of the glycine [19,23]. Figure 4a shows the selected range FT-IR spectra of the pure glycine and Gly@Al₂O₃ nanoparticles for better visualization and comparison. It is seen that the COO⁻ and CH₂ bands in the Gly@Al₂O₃ nanoparticles are blue shifted to higher wavenumber in comparison to pure glycine, which confirms the interaction of glycine with Al₂O₃ nanoparticles through COO⁻ group in accordance with earlier reports [19,23]. Further, the TGA curve of Gly@Al₂O₃ nanoparticles displays that nearly 50% glycine is attached to the Al₂O₃ nanoparticles, as seen from figure 4b. These results suggest that the Gly@Al₂O₃ nanoparticles should possess positive charge on the surface owing to the NH₃⁺ group in bi-functional glycine

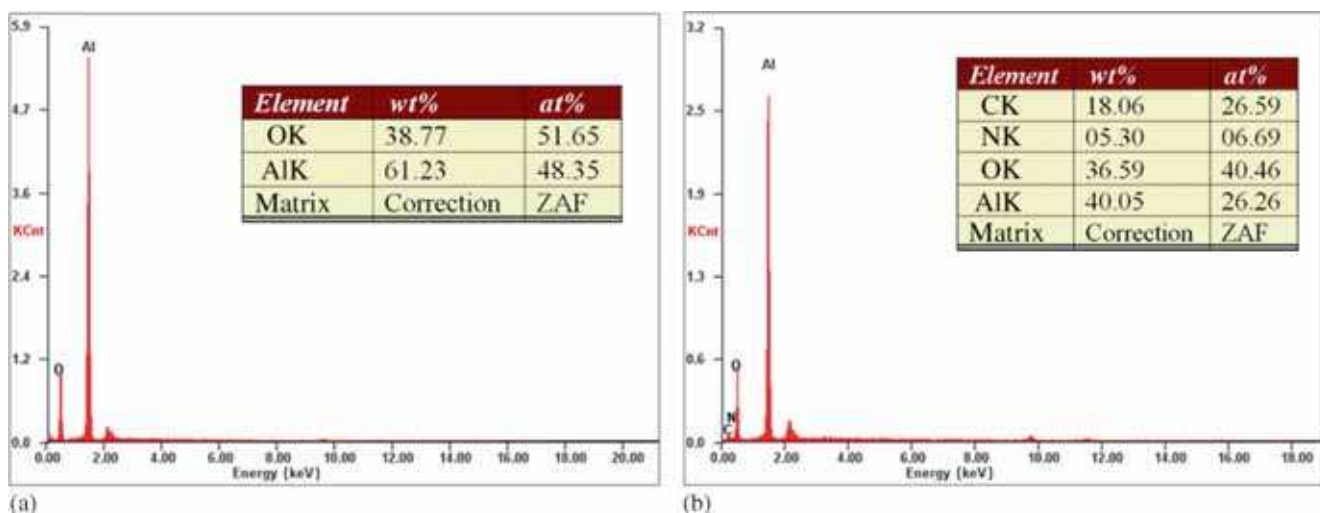


Figure 3. EDX spectra of (a) Al_2O_3 and (b) Gly@ Al_2O_3 nanoparticles.

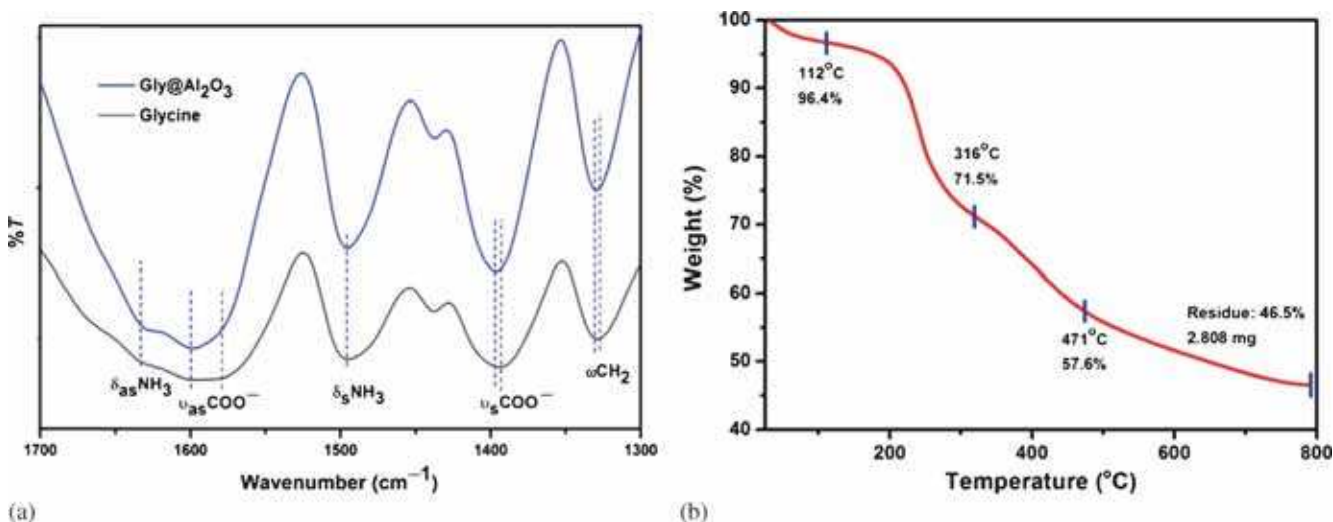


Figure 4. (a) Selected range FT-IR spectra of the pure glycine and Gly@ Al_2O_3 nanoparticles and (b) TGA curve of Gly@ Al_2O_3 nanoparticles.

molecule coated on the nanoparticles. Thus, it is expected that the NH_3^+ groups of glycine on the surface of Gly@ Al_2O_3 nanoparticles can interact with COO^- groups of side chain functional groups of collagen molecules through ionic or electrovalent linkages.

FT-IR spectra of collagen, collagen interacted with Al_2O_3 and Gly@ Al_2O_3 nanoparticles are shown in figure 5a. The characteristic amide I, amide II, and amide III bands of collagen are seen at 1645, 1540 and 1240 cm^{-1} , respectively. These bands are in agreement with the earlier report [25]. The peak broadening at 500–800 cm^{-1} for nanoparticle interacted samples is ascribed to the presence of alumina nanoparticles. In the collagen interacted with Gly@ Al_2O_3 nanoparticles, the glycine peaks are not distinctly visible especially those present between 500 and 1000 cm^{-1} . This may be due to the fact that collagen itself made up of several amino acids

including glycine and the amount of glycine coated on the interacted Gly@ Al_2O_3 nanoparticles is very low compared with collagen.

To understand the thermal stability of collagen nanocomposites prepared in ethanol medium, wet samples of collagen interacted with Al_2O_3 and Gly@ Al_2O_3 nanoparticles were analysed using DSC and the results are shown in figure 5b. It is well known that wet collagen shrinks irreversibly around 65 $^{\circ}\text{C}$ when heated in the presence of water, which is known as shrinkage temperature or hydrothermal stability [7]. The interaction of neat Al_2O_3 nanoparticles with collagen decreases the shrinkage temperature to 60 $^{\circ}\text{C}$ in spite of the use of ethanol medium in the place of water. It is known that aluminium reversibly reacts with collagen in water medium and it is washed out of treated skin matrix when soaked in water [7]. This may be the reason behind

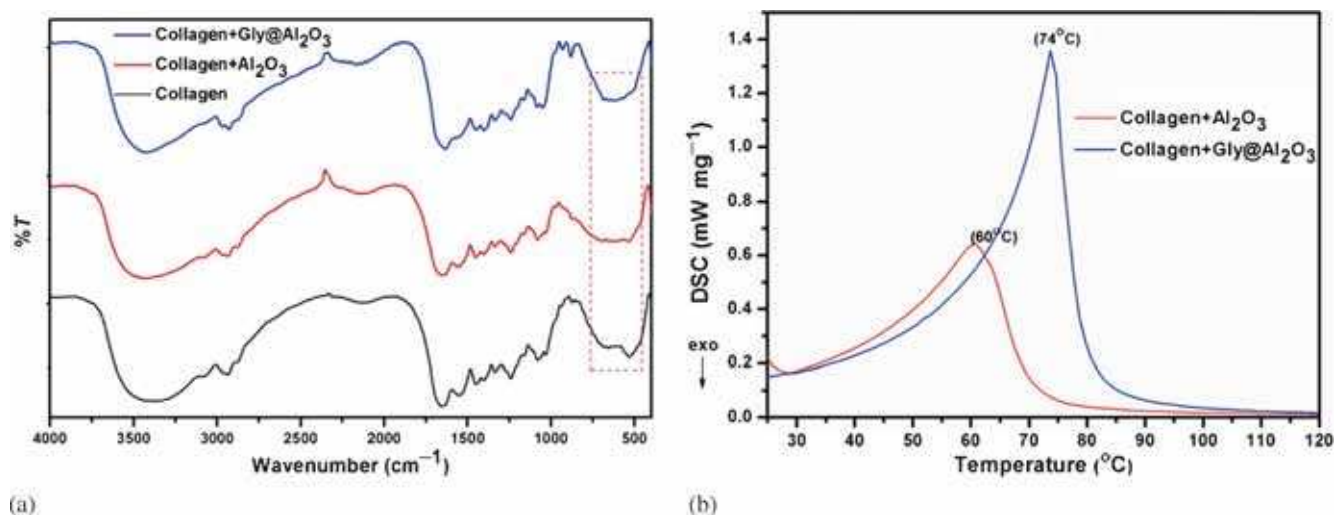


Figure 5. (a) FT-IR spectra and (b) DSC traces of collagen interacted with Al₂O₃ and Gly@Al₂O₃ nanoparticles.

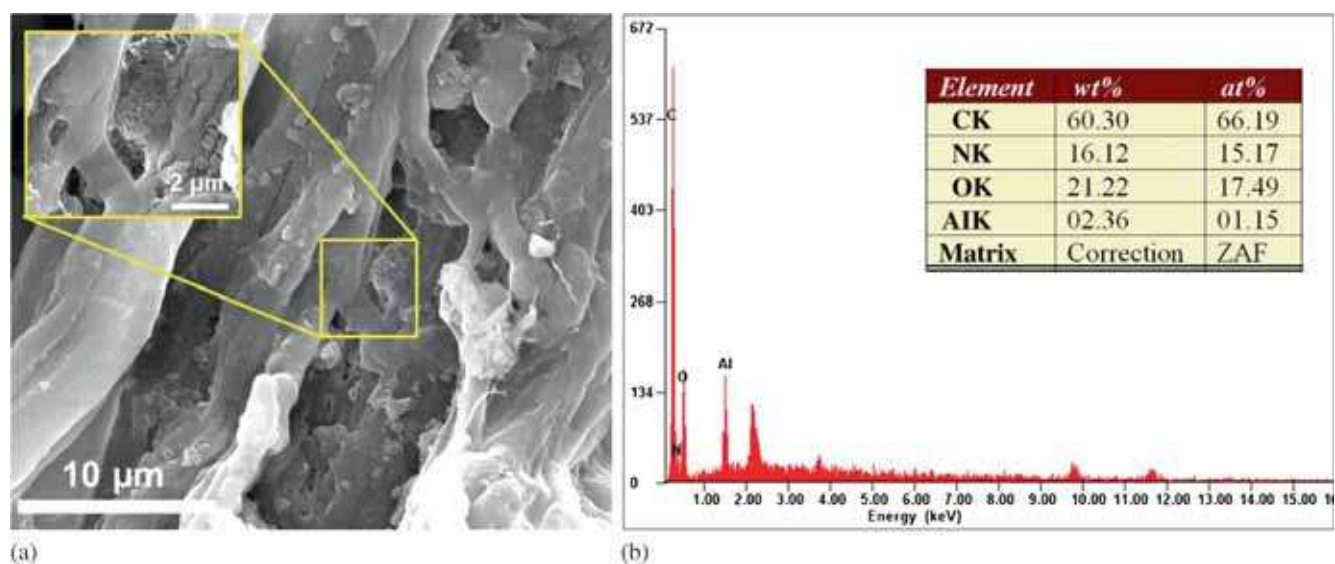


Figure 6. (a) HRSEM image and (b) EDX spectrum of collagen interacted with Gly@Al₂O₃ nanoparticles. Inset shows the magnified view of the select portion of figure 5a.

the low shrinkage temperature observed for the collagen treated with neat Al₂O₃ nanoparticles. However, Gly@Al₂O₃ nanoparticles increase the shrinkage temperature of collagen to 74°C as shown in figure 5b. This can be attributed to the ionic linkage of NH₃⁺ group in glycine molecule coated on the Gly@Al₂O₃ nanoparticles with the COO⁻ groups of side chain functional groups of collagen molecules as explained above. HRSEM image of the collagen interacted with Gly@Al₂O₃ nanoparticles is shown in figure 6a. It can be seen that the Gly@Al₂O₃ nanoparticles are present on the surface of the collagen fibres. The magnified view, seen as inset, from the selected portion of figure 6a substantiates this observation. The EDX spectrum of collagen interacted with Gly@Al₂O₃ nanoparticles also confirms the presence of aluminium-based nanoparticles on the surface of collagen (figure 6b).

4. Conclusion

In summary, alumina nanoparticle and glycine functionalized Al₂O₃ molecule having a bi-functional group were synthesized. XRD and FT-IR analysis reveal the presence of γ-Al₂O₃ and γ-glycine in the Gly@Al₂O₃ nanoparticles. HRSEM analysis shows that the Gly@Al₂O₃ nanoparticles are inter-connected rather than agglomerated unlike neat Al₂O₃ nanoparticles. The as-synthesized Al₂O₃ and Gly@Al₂O₃ nanoparticles were used to stabilize the collagen fibres. The results show that Gly@Al₂O₃ nanoparticles increase the thermal stability of collagen up to 74°C. The study reveals that the stabilization of collagen using Gly@Al₂O₃ nanoparticles has potential for applications in leather making, biomedicine and cosmetics.

Acknowledgements

Financial support from CSIR under XIIth plan project 'Research Initiatives for Waterless Tanning' (RIWT-CSC0202) is greatly acknowledged. CSIR-CLRI Communication no. 1156.

References

- [1] Ramachandran G N and Kartha G 1955 *Nature* **176** 593
- [2] Usha R and Ramasami T 1999 *Thermochim. Acta* **338** 17
- [3] Eyre D and Wu J-J 2005 *Collagen* (Berlin, Heidelberg: Springer) Vol 247, p 207
- [4] Chan B P and So K F 2005 *J. Biomed. Mater. Res. A* **75A** 689
- [5] Thanikaivelan P, Geetha V, Rao J R, Sreeram K J and Nair B U 2000 *J. Soc. Leather Technol. Chem.* **84** 82
- [6] Chakravorty H P and Nursten H E 1958 *J. Soc. Leather Technol. Chem.* **42** 2
- [7] Covington A D 1997 *Chem. Soc. Rev.* **26** 111
- [8] Raghava Rao J, Chandrababu N K, Muralidharan C, Nair B U, Rao P G and Ramasami T 2003 *J. Clean. Prod.* **11** 591
- [9] www.un.org, 2002
- [10] Krishnamoorthy G, Sadulla S, Sehgal P K and Mandal A B 2012 *J. Hazard. Mater.* **215–216** 173
- [11] Manfred R, Eckhard W, Björn J and Helmut G 2012 *J. Supercrit. Fluid* **66** 291
- [12] Mo X, An Y, Yun C-S and Yu S M 2006 *Angew. Chem. Int. Ed.* **45** 2267
- [13] Sisco P N, Wilson C G, Mironova E, Baxter S C, Murphy C J and Goldsmith E C 2008 *Nano Lett.* **8** 3409
- [14] Fan H, Li L, Shi B, He Q and Peng B 2005 *J. Am. Leather Chem. Assoc.* **100** 22
- [15] Thanikaivelan P, Narayanan N T, Pradhan B K and Ajayan P M 2012 *Sci. Rep.* **2** 230
- [16] Alliraja C, Rao J R and Thanikaivelan P 2015 *RSC Adv.* **5** 20939
- [17] Castaneda L, Valle J, Yang N, Pluskat S and Slowinska K 2008 *Biomacromolecules* **9** 3383
- [18] Gupta A K and Gupta M 2005 *Biomaterials* **26** 3995
- [19] Feitoza N C, Gonçalves T D, Mesquita J J, Menegucci J S, Santos M-K, Chaker J A, Cunha R B, Medeiros A M M, Rubim J C and Sousa M H 2014 *J. Hazard. Mater.* **264** 153
- [20] Pradhan A C, Parida K M and Nanda B 2011 *Dalton Trans.* **40** 7348
- [21] Ali Ahamed S Z, Dillip G R, Raghavaiah P, Mallikarjuna K and Deva Prasad Raju B 2013 *Arab. J. Chem.* **6** 429
- [22] Ma C, Chang Y, Ye W, Shang W and Wang C 2008 *J. Colloid. Interface Sci.* **317** 148
- [23] Tzvetkov G, Koller G, Zubavichus Y, Fuchs O, Casu M B, Heske C, Umbach E, Grunze M, Ramsey M G and Netzer F P 2004 *Langmuir* **20** 10551
- [24] Inagaki T, Aono S, Nakano H and Yamamoto T 2014 *J. Phys. Chem. B* **118** 5499
- [25] Song J-H, Kim H-E and Kim H-W 2007 *J. Biomed. Mater. Res. B* **83B** 248